

RESEARCH ARTICLE



Characterization of *Trichuris muris* secreted proteins and extracellular vesicles provides new insights into host–parasite communication

Ramon M. Eichenberger ^a, Md Hasanuzzaman Talukder ^b, Matthew A. Field ^a, Phurpa Wangchuk ^a, Paul Giacomini^a, Alex Loukas ^a and Javier Sotillo ^a

^aCentre for Biodiscovery and Molecular Development of Therapeutics, Australian Institute of Tropical Health and Medicine, James Cook University, Cairns, QLD, Australia; ^bFaculty of Veterinary Sciences, Bangladesh Agricultural University, Mymensingh, Bangladesh

ABSTRACT

Whipworms are parasitic nematodes that live in the gut of more than 500 million people worldwide. Owing to the difficulty in obtaining parasite material, the mouse whipworm *Trichuris muris* has been extensively used as a model to study human whipworm infections. These nematodes secrete a multitude of compounds that interact with host tissues where they orchestrate a parasitic existence. Herein we provide the first comprehensive characterization of the excretory/secretory products of *T. muris*. We identify 148 proteins secreted by *T. muris* and show for the first time that the mouse whipworm secretes exosome-like extracellular vesicles (EVs) that can interact with host cells. We use an Optiprep® gradient to purify the EVs, highlighting the suitability of this method for purifying EVs secreted by a parasitic nematode. We also characterize the proteomic and genomic content of the EVs, identifying >350 proteins, 56 miRNAs (22 novel) and 475 full-length mRNA transcripts mapping to *T. muris* gene models. Many of the miRNAs putatively mapped to mouse genes are involved in regulation of inflammation, implying a role in parasite-driven immunomodulation. In addition, for the first time to our knowledge, colonic organoids have been used to demonstrate the internalization of parasite EVs by host cells. Understanding how parasites interact with their host is crucial to develop new control measures. This first characterization of the proteins and EVs secreted by *T. muris* provides important information on whipworm–host communication and forms the basis for future studies.

ARTICLE HISTORY

Received 19 April 2017
Accepted 7 January 2018

KEYWORDS

extracellular vesicles;
exosomes; *Trichuris muris*;
whipworm; miRNA;
proteomics; organoids

Introduction

Infections with soil-transmitted helminths (STH) affect more than 1.5 billion people worldwide, causing great socio-economic impact as well as physical and intellectual retardation [1]. Among the STH, hookworms (*Necator americanus* and *Ancylostoma duodenale*), roundworms (*Ascaris lumbricoides*) and whipworms (*Trichuris trichiura*) are of particular importance, owing to their high prevalence and disease burden in impoverished countries [2]. For instance, *T. trichiura* alone infects around 500 million people worldwide, and contributes to 638,000 years of life lived with disability (YLDs) [2].


Infection with *Trichuris* spp. occurs after ingestion of infective eggs, which hatch in the caecum of the host. Larvae penetrate the mucosal tissue, where they moult to become adult worms and reside for the rest of their lives. Owing to the difficulty in obtaining parasite material to study whipworm infections, particularly

adult worms, the rodent whipworm, *Trichuris muris*, has been extensively used as a tractable model of human trichuriasis [3–5]. In addition to parasitologists, immunologists have also benefited from the study of *T. muris* infections, and a significant amount of basic immunology research has been conducted using this model (reviewed by [6]). For instance, the role of IL-13 in resistance to nematode infections was elucidated using *T. muris* [7].

The recent publication of the genome and transcriptome of *T. muris* has provided meaningful insights into the immunobiology of whipworm infections [8]. This work provided new information on potential drug targets against trichuriasis and elucidated important traits that drive chronicity. Despite this progress, and the tractability of the *T. muris* model, very few proteomic studies have been conducted, and only a handful of reports have described proteins secreted by *Trichuris* spp. [9–14]. Drake *et al.* characterized a pore-forming protein that *T. muris* [14] and *T. trichiura* [13] use to drill holes in

CONTACT Javier Sotillo  javier.sotillo@jcu.edu.au; Alex Loukas  alex.loukas@jcu.edu.au  Centre for Biodiscovery and Molecular Development of Therapeutics, James Cook University, Cairns, Queensland 4878, Australia

[†]These authors contributed equally to this work.

 Supplemental data for this article can be accessed [here](#).

© 2018 The Author(s). Published by Informa UK Limited, trading as Taylor & Francis Group

This is an Open Access article distributed under the terms of the Creative Commons Attribution-NonCommercial License (<http://creativecommons.org/licenses/by-nc/4.0/>), which permits unrestricted non-commercial use, distribution, and reproduction in any medium, provided the original work is properly cited.

the host cell membrane. Furthermore, it has been suggested that a thioredoxin-like protein secreted by the pig whipworm *Trichuris suis* plays a role in mucosal homeostasis [11].

The importance of excretory/secretory (ES) products in governing host–parasite interactions and ensuring parasite survival in inhospitable environments is indisputable. Traditionally, ES products were believed to contain only soluble proteins, lipids, carbohydrates and genomic content; however, the recent discovery of extracellular vesicles (EVs) secreted by helminths has revealed a new paradigm in the study of host–parasite relationships [15–17]. Helminth EVs have immunomodulatory effects and contribute to pathogenesis. For instance, EVs secreted by parasitic flatworms can promote tumorigenesis [18] and polarize host macrophages towards a M1 phenotype [19], while EVs from the gastrointestinal nematode *Heligmosomoides polygyrus* contain small RNAs that can modulate host innate immunity [20].

In the present study, we aim to characterize the factors involved in *T. muris*–host relationships. We provide the first proteomic analysis of the soluble proteins present in the ES products, and we describe the proteomic and nucleic acid content of EVs secreted by whipworms. This work provides important information on whipworm biology and contributes to the development of new strategies and targets to combat nematode infections in humans and animals.

Experimental procedures

Ethics statement

The study was approved by the James Cook University (JCU) Animal Ethics Committee (A2213). Mice were maintained at the JCU animal house (Cairns campus) under normal conditions of regulated temperature (22°C) and lighting (12 h light/dark cycle) with free access to pelleted food and water. The mice were kept in cages in compliance with the Australian Code of Practice for the Care and Use of Animals for Scientific Purposes.

Parasite material, isolation of ES products and EV purification

Parasites were obtained from genetically susceptible B10.BR mice infected with 200 *T. muris* eggs. The infection load (200 *T. muris* eggs per mouse) is well tolerated and results, usually, in ~180 adult parasites/mouse (90% success). Adult worms were harvested from the caecum of infected mice 5 weeks after infection, washed in PBS containing 5× antibiotic/antimycotic (AA) and cultured in six-well plates for 5 days in RPMI containing 1× AA, at

37°C and 5% CO₂. Each well contained ~500 worms in 4.5 ml media. The media obtained during the first 4 h after parasite culturing were discarded for further analysis. Dead worms were removed, and ES products were collected daily, subjected to sequential differential centrifugation at 500 g, 2000 g and 4000 g for 30 min each to remove eggs and parasite debris. For the isolation of ES products, media were concentrated using a 10 kDa spin concentrator (Merck Millipore, Burlington, MA, USA) and stored at 1.0 mg/ml in PBS at –80°C until required.

For the isolation of EVs, the media obtained after differential centrifugation were processed as described previously [21]. Briefly, ES products were concentrated using a 10 kDa spin concentrator, followed by centrifugation for 45 min at 12,000 g to remove larger vesicles. A MLS-50 rotor (Beckman Coulter, Brea, CA, USA) was used to ultracentrifuge the supernatant for 3 h at 120,000 g, and the resultant pellet was resuspended in 70 µl of PBS and subjected to Optiprep® discontinuous gradient (ODG) separation. One millilitre of 40%, 20%, 10% and 5% iodixanol solutions prepared in 0.25 M sucrose, 10 mM Tris-HCl, pH 7.2, was layered in decreasing density in an ultracentrifuge tube, and the 70 µl containing the resuspended EVs was added to the top layer and ultracentrifuged at 120,000 g for 18 h at 4°C. Seventy microlitres of PBS was added to the control tube prepared as described above. A total of 12 fractions were recovered from the ODG, and the excess Optiprep® solution was removed by buffer exchanging with 8 ml of PBS containing 1× EDTA-free protease inhibitor cocktail (Santa Cruz, Dallas, TX, USA) using a 10 kDa spin concentrator. The absorbance (340 nm) was measured in each of the fractions, and density was calculated using a standard curve with known standards. The protein concentration of all fractions was measured using a Pierce BCA Protein Assay Kit (ThermoFischer, Waltham, MA, USA). All fractions were kept at –80°C until use.

Size and concentration analysis of EVs

The size distribution and particle concentration of fractions recovered after ODG were measured using tunable resistive pulse sensing (TRPS) by qNano (Izon, Christchurch, New Zealand) following the manufacturer's instructions. Voltage and pressure values were set to optimize the signal to ensure high sensitivity. A nanopore NP100 was used for all fractions analysed except for fraction 9, where a NP150 was used. Calibration was performed using CP100 carboxylated polystyrene calibration particles (Izon) at a 1:1000 dilution. Samples were diluted 1:5 and applied to the nanopore. The size and concentration of particles

were determined using the software provided by Izon (version 3.2).

Exosome uptake in murine colonic organoids (mini-guts)

Murine colonic organoids were produced from intestinal crypts of a female C57 Bl6/J mouse according to previous reports [22] with some modifications. Briefly, murine colonic crypts were dissociated with Gentle Cell Dissociation reagent (Stemcell Technology Inc., Vancouver, Canada) and further incubated in trypsin (ThermoFischer). Approximately 500 crypts were seeded in 50 μ l of Matrigel (Corning, NY, USA) in a 24-well plate and cultured in Intesticult Organoid Growth Medium (Stemcell Technology Inc.) supplemented with 100 ng/ml murine recombinant Wnt3a (Peprotech, Rocky Hill, NJ, USA). ROCK-inhibitor (10 μ M Y-27,632; Sigma-Aldrich, St. Louis, MO, USA) was included in the culture medium for the first 2 days to avoid anoikis.

For imaging, organoids were seeded in 75 μ l of Matrigel in six-well plates and cultured for 7 days. To investigate internalization of EVs in the colonic epithelium layer, EVs were labelled with PKH26 (Sigma-Aldrich) according to the manufacturer's instructions. A total of 15–30 million stained particles (based on the TRPS results) in 3–5 μ l were injected into the central lumen of individual organoids and cultured for 3 h at 37°C and 4°C, respectively. Cell-culture medium was removed, and wells were washed with PBS. Organoids were fixed by directly adding 4% paraformaldehyde to the six-well plates and incubating for 30 min at room temperature (RT). Matrigel was then mechanically disrupted, and cells were transferred into BSA-coated tubes. Autofluorescence was quenched by incubating the organoids with 50 mM NH₄Cl in PBS (for 30 min at RT) and 100 mM glycine in PBS (for 5 min). Cell nuclei were stained with Hoechst dye (Invitrogen, Carlsbad, CA, USA) and visualized on an AxioImager M1 ApoTome fluorescence microscope (Zeiss, Oberkochen, Germany). Fluorescence intensity of PKH26-stained parasite EVs was quantified in ImageJ and expressed as a percentage of corrected total fluorescence (% CTF) adjusted by background fluorescence and the surveyed area in total epithelial cells (donut-shaped selection) or in the lumen incubated at different conditions in 10 different murine colonic organoids from two technical replicates (five each). The whole experiment was repeated to perform laser scanning confocal imaging on a 780 NLO microscope (Zeiss). Confocal image deconvolution was performed in ImageJ using the plugins “Diffraction PSF 3D” for PSF calculation and “DeconvolutionLab” with the Richardson–Lucy algorithm for 3D deconvolution and Tikhonov–Miller algorithm for 2D deconvolution [23].

Proteomic analyses

The protein contents from the *T. muris* ES products and ODG fractions were analysed as follows.

Proteomic analysis of ES products

One hundred micrograms (100 μ g) of *T. muris* ES proteins from two different batches of adult worms were precipitated at –20°C overnight in ice-cold methanol. Proteins were resuspended in 50 mM NH₄HCO₃, reduced in 20 mM dithiothreitol (DTT, Sigma-Aldrich) and finally alkylated in 55 mM iodoacetamide (IAM, Sigma-Aldrich). Proteins were finally digested with 2 μ g of trypsin (Sigma-Aldrich) by incubating for 16 h at 37°C with gentle agitation. Reaction was stopped with 5% formic acid, and the sample was desalted using ZipTip® (Merck Millipore). Both samples were kept at –80°C until use.

Proteomic analysis of EVs

For the proteomic analysis of EVs, two replicates were analysed independently. The ODG fractions with a density of 1.07–1.09 g/ml (fractions 5–7) were combined, and a total of 50 μ g of protein from each of the two replicates was loaded on a 12% SDS-PAGE and electrophoresed at 100 V for 1.5 h. Each lane was sliced into nine pieces, which were subjected to trypsin digestion as described previously [24]. Briefly, each slice was washed for 5 min three times in 50% acetonitrile, 25 mM NH₄CO₃ and then dried under a vacuum centrifuge. Reduction was carried out in 20 mM DTT for 1 h at 65°C, after which the supernatant was removed. Samples were then alkylated in 55 mM IAM at RT in darkness for 40 min. Gel slices were then washed 3 \times in 25 mM NH₄CO₃ before drying in a vacuum centrifuge followed by digestion with 500 ng of trypsin overnight at 37°C. The digest supernatant was removed from the gel slices, and residual peptides were removed from the gel slices by washing three times with 0.1% TFA for 45 min at 37°C. Samples were desalted and concentrated using Zip-Tip® and kept at –80°C until use.

Mass spectrometry and database searches

For all analyses, samples were reconstituted in 10 μ l of 5% formic acid. Six microlitres of sample was injected onto a 50 mm 300 μ m C18 trap column (Agilent Technologies, Santa Clara, CA, USA) and desalted for 5 min at 30 μ L/min using 0.1% formic acid (aq). Peptides were then eluted onto an analytical nano HPLC column (150 mm \times 75 μ m 300SBC18, 3.5 μ m, Agilent Technologies) at a flow rate of 300 nL/min and separated using a 35 min gradient (for ES proteins) or

95 min gradient (for EV proteins) of 1–40% buffer B (90/10 acetonitrile/0.1% formic acid) followed by a steeper gradient from 40 to 80% buffer B in 5 min. The 5600 mass spectrometer operated in information-dependent acquisition mode, in which a 1 s TOF-MS scan from 350–1400 m/z was performed, and for product ion ms/ms 80–1400 m/z ions observed in the TOF-MS scan exceeding a threshold of 100 counts and a charge state of +2 to +5 were set to trigger the acquisition of product ion. Analyst 1.6.1 (ABSCIEX, Framingham, MA, USA) software was used for data acquisition and analysis.

For the analysis of the ES products, a database was built using the *T. muris* genome [8] with the common repository of adventitious proteins (cRAP, <http://www.thegpm.org/crap/>) appended to it. A similar database containing the *T. muris* genome, the cRAP and the *Mus musculus* genome was used for the analysis of the EV mass spectrometry data. Database search was performed using X!Tandem, MS-GF+, OMSSA and Tide search engines using SearchGUI [25]. Parameters were set as follows: tryptic specificity allowing two missed cleavages, MS tolerance of 50 ppm and 0.2 Da tolerance for MS/MS ions. Carbamidomethylation of Cys was used as fixed modification and oxidation of Met and deamidation of Asn and Gln as variable modifications. PeptideShaker v.1.16.15 was used to import the results for peptide and protein inference [26]. Peptide-Spectrum Matches (PSMs), peptides and proteins were validated at a 1.0% False Discovery Rate estimated using the decoy hit distribution. Only proteins having at least two unique peptides (containing at least seven amino acid residues) were considered as positively identified. The mass spectrometry proteomics data have been deposited to the ProteomeXchange Consortium via the PRIDE partner repository with the dataset identifier PXD008387 (for the extracellular vesicles data) and PXD006344 (for the ES products data).

RNA analyses

mRNA and miRNA isolation

Two different biological replicates of EVs obtained from two different batches of worms were used. ODG fractions with a density between 1.07 and 1.09 (fractions containing pure EV samples after TRPS analysis) were pooled, and excess Optiprep® solution was removed by buffer exchanging. Total RNA and miRNA were extracted using the mirVana™ miRNA Isolation Kit (ThermoFischer) according to the manufacturer's instructions. RNA was eluted over two fractions of 50 μ l each and stored at -80°C until analysed.

RNA sequencing and transcript annotation

The RNA quality, yield and size of total and small RNAs were analysed using capillary electrophoresis (Agilent 2100 Bioanalyzer, Agilent Technologies, USA). Ribosomal RNA was removed from samples, which were pooled for sufficient input material for further sequencing, resulting in one sample for mRNA and two replicates for miRNA analyses, respectively. mRNA and miRNA were prepared for sequencing using Illumina TruSeq stranded mRNA-seq and Illumina TruSeq Small RNA-seq library preparation kit according to the manufacturer's instructions, respectively. RNAseq was performed on a HiSeq 500 (Illumina, single-end 75-bp PE mid output run, approx. 30M reads per sample). Quality control, library preparation and sequencing were performed at the Ramaciotti Centre for Genomics at the University of New South Wales. The data have been deposited in NCBI's Gene Expression Omnibus and are accessible through GEO Series accession numbers GSE107985 and GSE107986.

Bioinformatic analyses

Proteomics

Proteins were classified according to Gene Ontology (GO) categories using the software Blast2GO basic version 4.0.7 [27] and Pfam using HMMER v3.1b1 [28]. Putative signal peptides and transmembrane domain(s) were predicted using the programs CD-Search tool [29] and SignalP [30].

mRNA analysis

High-throughput RNA-seq data were aligned to the *T. muris* reference genome models (WormBase WS255; <http://parasite.wormbase.org>; [31]) using the STAR transcriptome aligner [32]. Prior to downstream analysis, rRNA-like sequences were removed from the metatranscriptomic dataset using riboPicker-0.4.3 (<http://ribopicker.sourceforge.net>; [33]). BLASTn algorithm [34] was used to compare the non-redundant mRNA dataset for *T. muris* EVs to the nucleotide sequence collection (nt) from NCBI (www.ncbi.nlm.nih.gov) to identify putative homologues in a range of other organisms (cutoff: $<1\text{E-}03$). Corresponding hits homologous to the murine host, with a transcriptional alignment coverage $<95\%$ (based on the effective transcript length divided by length of the gene), and with an expression level <10 fragments per kilobase of exon model per million mapped reads (FPKM) normalized by the length of the gene, were removed from the list. The final list of mRNA transcripts from *T. muris* exosomes was assigned to protein families (Pfam) and GO categories (Blast2GO).

miRNA analysis and target prediction

The miRDeep2 package [35] was used to identify known and putative novel miRNAs present in both miRNA samples. As there are no *T. muris* miRNAs available in miRBase release 21 [36], the miRNAs from the nematodes *Ascaris suum*, *Brugia malayi*, *Caenorhabditis elegans*, *Caenorhabditis brenneri*, *Caenorhabditis briggsae*, *Caenorhabditis remanei*, *Haemonchus contortus*, *Pristionchus pacificus*, *Panagrellus redivivus* and *Strongyloides ratti* were utilized as a training set for the algorithm. Only miRNA sequences commonly identified in both replicates were included for further analyses. The interaction between miRNA and murine host genes was predicted using the miRanda algorithm 3.3a [37]. Input 3'UTR from the *M. musculus* GRCm38.p4 assembly was retrieved from the Ensembl database release 86 [38]. The software was run with strict 5' seed pairing, energy threshold of -20 kcal/mol and default settings for gap open and gap extend penalties. Interacting hits were filtered by conservative cutoff values for pairing score (>155) and matches ($>80\%$). The resulting gene list was classified by the Panther classification system (<http://pantherdb.org/>) using pathway classification [39] and curated by the reactome pathway database (www.reactome.org) [40].

Results

Proteomics analysis of the ES products of *T. muris*

The ES products secreted by two different batches of *T. muris* adult worms were analysed using LC-MS/MS. A total of 1777 and 2056 PSMs were confidently identified in the first and second biological replicates analysed respectively. Similarly, a total of 591 and 704, corresponding to 197 and 233 proteins, were identified with 100% confidence. After removing the proteins identified from only one peptide and the sequences belonging to the contaminants, 100 and 116 *T. muris* proteins were identified in both replicates. A total of 68 proteins were found in both replicates, whereas 32 and 48 proteins were uniquely found in replicate 1 and 2 respectively, resulting in 148 proteins in total (Supplementary Table 1).

The identified proteins were subjected to a Pfam and GO analysis. The most represented domains were “trypsin-like peptidase”, “thioredoxin-like” and “tetra-tricopeptide repeat domains”, with 21, 19 and 13 proteins containing these domains respectively (Figure 1(a)). The most abundant GO terms within the “molecular function” ontology were “protein binding”, “metal ion binding” and “nucleic acid” as well as “isomerase activity”, “oxidoreductase activity” and “serine-type peptidase activity” (Figure 1(b)). The GO terms within “biological process” and “cell component” (as

well as the above-mentioned “molecular function”) are detailed in Supplementary Table 1.

From the total of 148 proteins found in both replicates, only 62 had a signal peptide (Supplementary Table 2), which opened the possibility of other non-classical mechanisms of secretion of these proteins described in other helminths, such as EVs.

T. muris adult worms secrete exosome-like EVs that can be internalized by host cells

The ES products secreted by *T. muris* adult worms were concentrated and EVs purified using Optiprep® gradient. The density of the 12 fractions recovered after Optiprep® separation was measured, ranging from 1.04 to 1.27 g/ml (Table 1). All fractions were subjected to TRPS analysis using a qNano system, but only fractions 4–10 contained enough vesicles for the analysis (Figure 2). Fraction 6 (corresponding to a density of 1.07 g/ml) contained the highest number of EVs (1.34×10^{12} particles/ml), followed by fraction 7 (density = 1.008 g/ml; concentration = 8.21×10^{10} particles/ml) and fraction 5 (density = 1.07 g/ml; concentration = 7.47×10^{10}) (Table 1). Protein concentration was measured in all fractions, and EV purity determined as described previously [41] (Table 1). Fraction 6 had the purest EV preparation (4.31×10^9 particles/ μ g), followed by fractions 7 and 5 (4.04×10^8 and 1.58×10^8 particles/ μ g respectively) (Table 1). Furthermore, the vesicle size was determined using the qNano system, and the results are summarized in Table 1.

In vitro cellular uptake of *T. muris* EVs in host cells was studied using murine colonic organoids, comprising the complete census of progenitors and differentiated cells from the colon epithelial tissue growing in cell culture. Purified membrane-labelled *T. muris* EVs were injected into the central lumen of the colonic organoids (corresponding to the intestinal lumen), and they were incubated for 3 h at 37°C to demonstrate cellular uptake. We observed internalization of EVs by organoid cells, which was absent by preventing endocytosis in metabolic inactive cells at 4°C (Figure 3). Using confocal microscopy, we confirmed that EVs were inside cells and present a cytoplasmic location of the stained EVs in some cells within the donut-shaped epithelial layer. By analysing the pictures and comparing the area of epithelial cells and the central lumen, uptake of stained vesicles at 37°C could be quantitatively traced within epithelial organoid cells (mean % CTF \pm SD: 4.04 ± 1.11), and % CTF values were significantly reduced ($p < 0.001$) in the central lumen (0.59 ± 0.41), whereas at 4°C, CTF values were 0.21 ± 0.29 and 3.79 ± 2.29 for the total epithelial organoid cells and the central lumen, respectively (Figure 3(e)).

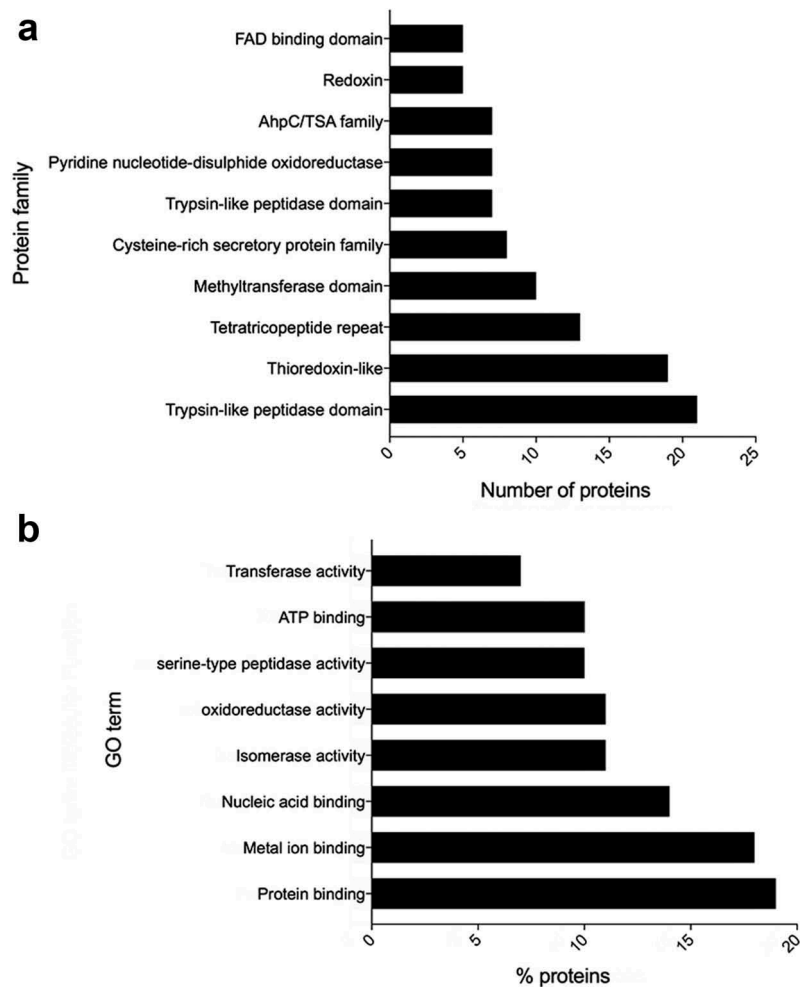


Figure 1. Bioinformatic analyses of the proteins secreted by *Trichuris muris*. (a) Bar graph showing the most abundant protein families after a Pfam analysis on the excretory/secretory proteins derived from *T. muris*. (b) Bar graph showing the most abundantly represented gene ontology molecular function terms in excretory/secretory proteins derived from *T. muris*.

Table 1. Features of the different fractions isolated after Optiprep fractionation of extracellular vesicles from *Trichuris muris*. Despite protein being detected in all fractions, only vesicles from fractions 4–10 could be quantified. The purity of the different fractions was calculated according to Webber and Clayton [41].

Optiprep fraction	Density (g/ml)	Protein quantification (µg/ml)	Particle concentration (particles/ml)	Purity of vesicles particles/µg	Particle size nm
S1	1.04	104.69	–	–	–
S2	1.05	290.10	–	–	–
S3	1.05	435.58	–	–	–
S4	1.06	477.86	2.96E + 08	6.19E + 05	93 ± 41.5
S5	1.07	474.19	7.47E + 10	1.58E + 08	72 ± 11.7
S6	1.07	310.61	1.34E + 12	4.31E + 09	72 ± 23.8
S7	1.08	202.99	8.21E + 10	4.04E + 08	90 ± 25.5
S8	1.10	160.76	1.31E + 10	8.15E + 07	152 ± 75.3
S9	1.12	190.46	1.31E + 10	6.88E + 07	183 ± 68.2
S10	1.15	436.86	1.71E + 09	3.91E + 06	165 ± 54.9
S11	1.21	232.77	–	–	–
S12	1.27	83.35	–	–	–

T. muris secreted EVs contain specific proteins

Two replicates containing ODG fractions with a density between 1.07 and 1.09 g/ml were subjected to SDS-PAGE separation, each lane cut into nine slices and subjected to

trypsin digestion followed by LC-MS/MS analysis. The results obtained from both replicates were combined, and only proteins commonly found in both replicates were considered for further analysis. A total of 28,376 and

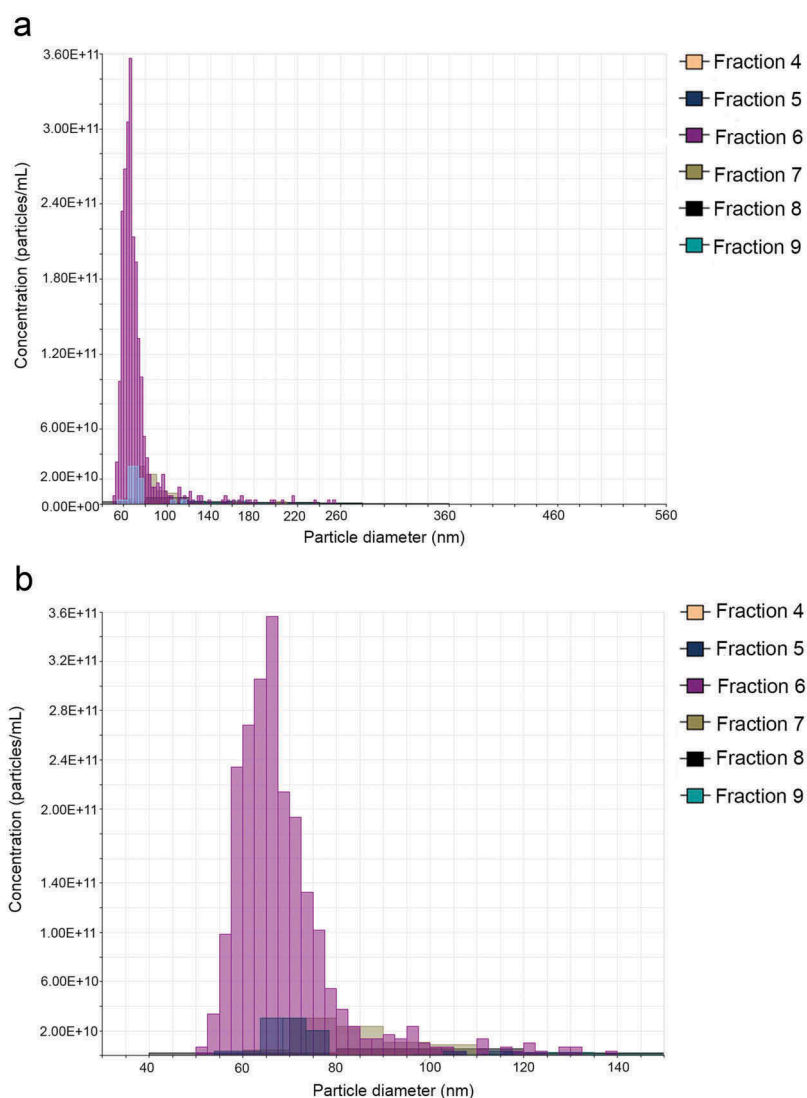


Figure 2. Tunable resistive pulse sensing analysis of the extracellular vesicles (EVs) secreted by *Trichuris muris*. (a) Size and number of the EVs secreted by *T. muris* after purification using an Optiprep® gradient was analysed using a qNano system (iZon). (b) Detailed graph showing number of vesicles with a diameter between 30 and 150 nm. Only fractions 4–9 contained enough vesicles for the analyses.

19,510 spectra corresponding to 6489 and 5455 peptides were identified in replicates 1 and 2 respectively. A total of 663 and 718 proteins matching *T. muris*, *M. musculus* and common contaminants for the cRAP database were identified (Supplementary Table 3). From these, 465 and 26 proteins containing at least two validated unique peptides matched *T. muris* and *M. musculus* respectively in replicate 1. Similarly, 486 and 36 proteins containing at least two validated unique peptides matched *T. muris* and *M. musculus* respectively in replicate 2. A final list of 364 and 17 proteins corresponding to *T. muris* and *M. musculus* respectively was defined with proteins commonly identified in both replicates (Supplementary Table 4). Only these common proteins were used in subsequent analyses

Among the identified proteins from *T. muris*, the most abundant proteins based on the spectrum count were a

trypsin domain-containing protein, several sperm-coating protein (SCP)-like extracellular proteins, also called SCP/Tpx-1/Ag5/PR-1/Sc7 domain-containing proteins (SCP/TAPS), a poly-cysteine and histidine-tailed protein, a glyceraldehyde-3-phosphate dehydrogenase and a TB2/DP1 HVA22 domain-containing protein. One tetraspanin (TMUE_s0037005100) was found in the EVs sample, as well as other proteins typically found in EVs from helminths like 14-3-3; heat shock protein (HSP) and glutathione-S-transferase were also identified in this study. Furthermore, from the 364 identified proteins from *T. muris*, only 50 (13.7%) contained a transmembrane domain, and 120 (32.96%) had a signal peptide. Despite washing the worms extensively before culturing, discarding the first 4 h of the ES for EV isolation (which typically contains a significant amount of host proteins) and

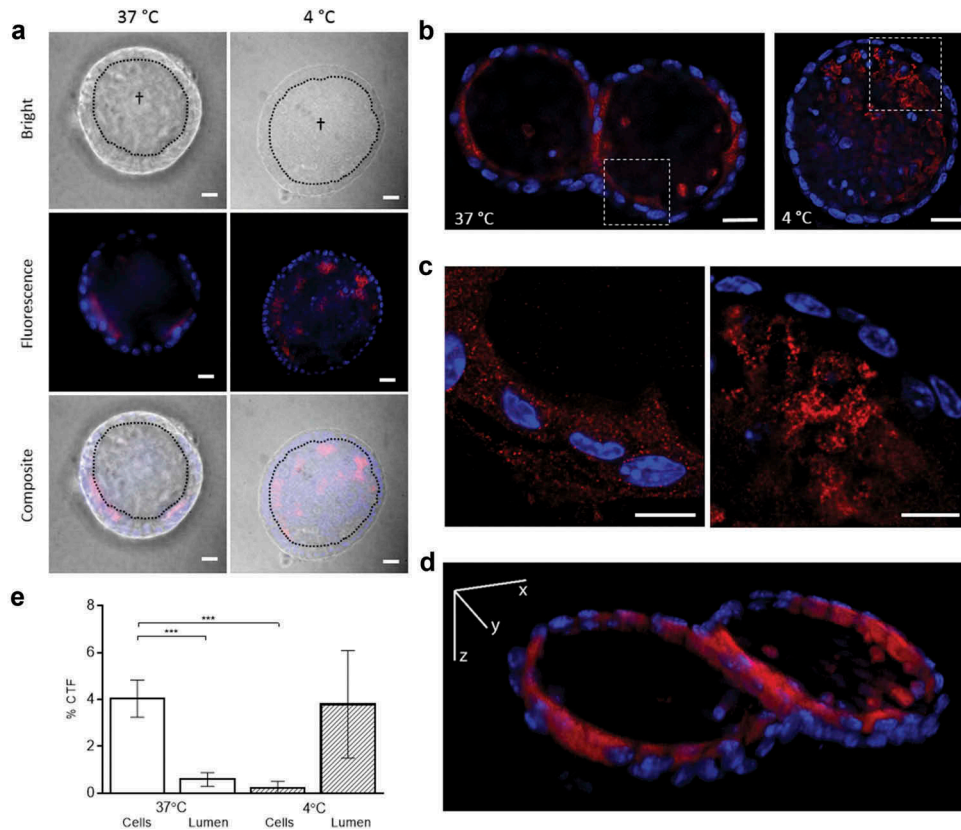


Figure 3. *Trichuris muris* extracellular vesicles (EVs) are internalized by murine colonic organoids. (a) Representative fluorescence images (Zeiss AxioImager M1 ApoTome) of PKH26-labelled EVs (red) internalized by organoids after 3 h at 37°C and 4°C (metabolically inactive cells). Hoechst dye (blue) was used to label cell nuclei. †Lumen of the organoids, which corresponds to the murine gut lumen, separated by the dotted line from the epithelial cell layer. White bar corresponds to 20 µm. (b) Deconvolved laser scanning confocal microscopy images (Zeiss 780 NLO) of murine colonic organoids under 20× magnification. White bar corresponds to 20 µm. (c) Magnification of the framed area in B under 100× magnification. White bar corresponds to 10 µm. (d) 3D projection of z-stack serial confocal images of a 12 µm organoid slice incubated with PKH26-labelled EVs after 3 h at 37°C (videos of 3D projections of the experiments at 37°C and 4°C are available in the supplementary materials). (e) Percentage of the CTF adjusted by background fluorescence and the surveyed area of PKH26-stained EVs in total epithelial cells (donut-shaped selection) or in the organoid lumen incubated under different conditions in 10 different organoids from two technical replicates (five each). ***Highly significant results ($p < 0.001$). Error bars indicate 95% confidence intervals.

analysing only fractions containing highly pure EV samples, we found some host proteins in our analysis. Among these proteins, we found an antibody Fc fraction and nine proteasome proteins (Supplementary Table 4).

Following a GO analysis, the most represented GO terms within biological process in the *T. muris* EV proteins were assigned as “cellular metabolic process”, “response to stimulus” and “proteolysis” (Figure 4(a)). Similarly, the most represented GO terms within molecular function were “oxidoreductase activity”, “protein binding” and “ATP binding” (Figure 4(b)).

T. muris secreted EVs contain specific mRNAs and miRNAs

RNA content of EVs was characterized using the Illumina HiSeq platform. For an initial description of parasite-

specific mRNAs in EVs, total RNA from a highly pure EV sample was sequenced, and results were curated based on stringent thresholds. This resulted in 475 full-length mRNA transcripts mapping to *T. muris* gene models. The identified hits were subjected to a Pfam and GO analysis. Interestingly, the most represented domains were of “unknown function”, “reverse transcriptase” and “helicase”, whereas other gene models with DNA-binding and processing domains were also highly abundant (e.g. genes with “retrotransposon peptidase” domain) (Figure 5(a)). Mapping to molecular functions identified “protein binding” as the most abundant term, with 31.9% of all sequences involved in this function (Figure 5(b)). The underlying proteins from the parasite-specific mRNAs had functions in signalling and signal transduction, transport, protein modification and biosynthetic processes, as well as in RNA processing and DNA integration (Figure 5(c)). Data are provided in Supplementary Table 5.

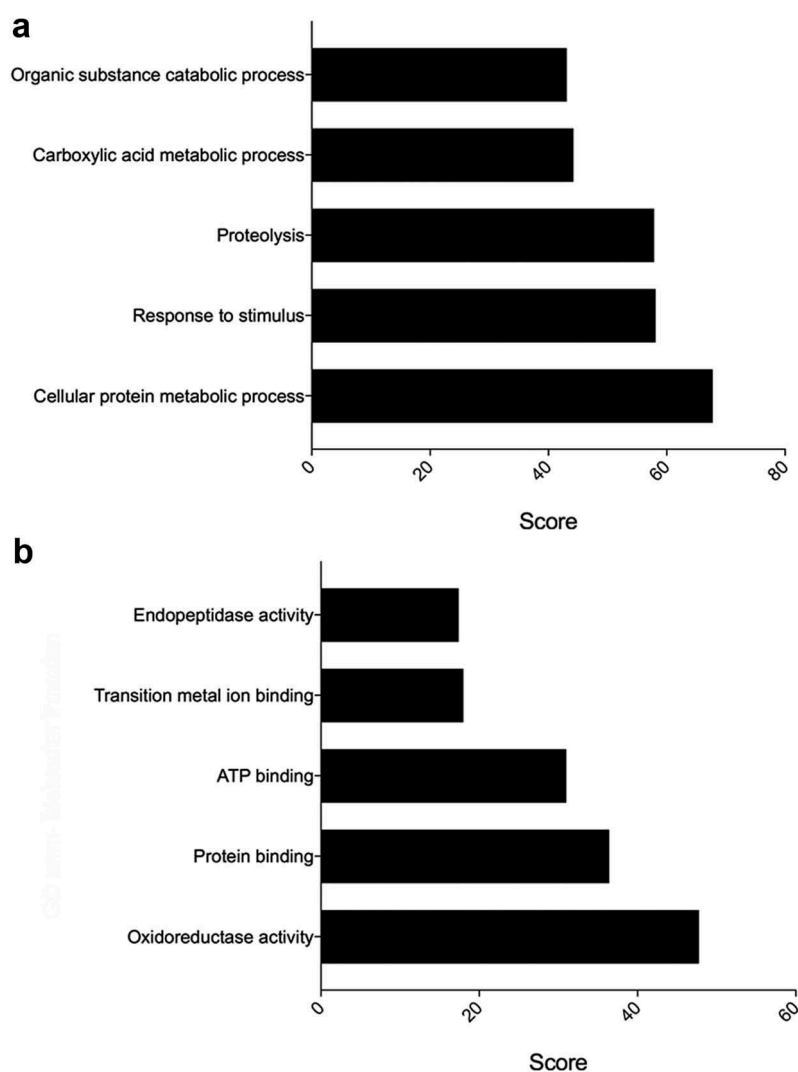


Figure 4. Gene ontology analysis of proteins from the extracellular vesicles (EVs) secreted by *Trichuris muris*. (a) Bar graph showing the most abundantly represented gene ontology biological process terms in proteins present in the EVs secreted by *T. muris*. (b) Bar graph showing the most abundantly represented gene ontology molecular function terms in proteins present in the EVs secreted by *T. muris*.

By sequencing and screening biological duplicates for miRNAs, we identified 56 miRNAs commonly present in both datasets, 34 of which have close homologues in other nematodes. The remaining 22 miRNAs were novel and were named serially according to their mean abundances (tmu.miR.ev1 to tmu.miR.ev22). Potential interactions of *T. muris* miRNAs to murine host genes were explored by computational target prediction. The 56 nematode EV miRNAs were predicted to interact with 2,043 3'UTR binding sites of the mouse genome assembly (Supplementary Table 6). Associated annotated coding genes were grouped according to signalling, metabolic, and disease pathways (Supplementary Figure 1). Indeed, a number of the nematode miRNA-mouse gene interactions are involved in host immune system, receptor and transcriptional regulation (Figure 6). Within the 56

identified EV miRNAs, three (5.4%) could not be assigned for interaction with a specific pathway in the murine host, including the second most abundant asu-miR-5360-5p.

Discussion

Trichuriasis is a soil-transmitted helminth infection that affects almost 500 million people worldwide [1,42,43]. In addition to the pathogenicity associated with the disease, the infection can also cause physical and intellectual retardation [1,44]. There is, therefore, an urgent need to understand the mechanisms by which the parasite interacts with its host such that novel approaches to combat this neglected tropical disease can be developed [45]. *T. trichiura* is the main species that affects humans,

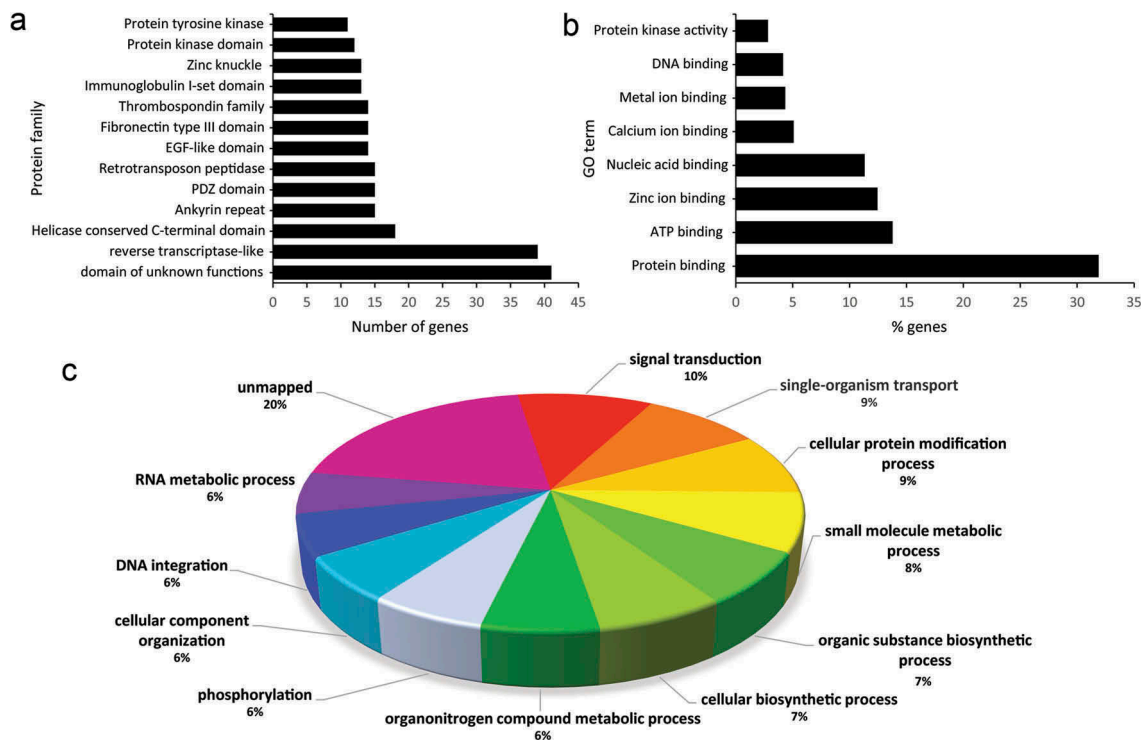


Figure 5. Analysis of the 475 full-length mRNAs detected in *Trichuris muris* extracellular vesicles. (a) Bar graph showing the most represented protein families (Pfam) from the translated mRNAs. (b) Molecular functions and (c) biological functions of proteins encoded by each of the 475 transcripts assigned to gene ontology functional annotation.

but the difficulty in obtaining worms and working with the adult stage has prompted parasitologists and immunologists to use the *T. muris* rodent model.

We provide herein the first high-throughput study of the secretome of *T. muris*. The analysis of the genome from *T. muris* predicted 434 proteins containing signal peptides [8]. We have confidently identified (with two or more peptides) 148 proteins secreted by adult *T. muris*, corresponding to 34.1% of the total predicted secreted proteins [8]. From the total proteins identified, 68 were commonly found in both replicates, highlighting the importance of analysing multiple batches of samples when conducting proteomics analyses of parasitic ES products. Among the identified proteins, we found several peptidases and proteases (such as serine proteases, pepsin and trypsin domain-containing proteins) and also protease inhibitors including WAP domain-containing proteins. These findings are in agreement with the functional annotation of the *T. muris* proteins predicted from the genome [8]. Protease inhibitors (particularly serine protease inhibitors and secretory leukocyte proteinase inhibitor (SLPI)-like proteins – proteins containing mostly WAP domains) are abundantly represented in the *T. muris* genome [8]. SLPI-like proteins have been suggested to have immunomodulatory properties as well as a role in wound healing [8,46–48], so they could be secreted in an attempt to modulate the host's immune

response and repair damage caused by both feeding/migrating worms and immunopathogenesis. In addition, we found five SCP/TAPS (also known as CAP-domain) proteins. SCP/TAPS proteins are abundantly represented in STH, although they have not been well characterized in the clade I nematodes [49].

Only recently, different authors have shown the importance of helminth-secreted EVs in host–parasite interactions. The secretion of small EVs was demonstrated in various intracellular and extracellular parasites, interacting with their hosts in a specific manner [17]. In addition, the secretion of EVs has been demonstrated thus far only in a small number of nematodes, including the free-living *C. elegans*, the filarial nematodes *Brugia malayi* and *Dirofilaria immitis*, the rodent nematode *Heligmosomoides polygyrus* and the ovine and porcine intestinal nematodes *Teladorsagia circumcincta* and *Trichuris suis*, respectively [20,50–53].

Our results show that *T. muris* secretes EVs with a wide variety of sizes (40–550 nm). In order to study the exosome-like vesicles (vesicles with a size between 50–150 nm) and eliminate contamination with soluble proteins that could be co-precipitated in the ultracentrifugation step, we further purified the EVs using Optiprep and analysed only fractions 5–7 (fractions containing EVs with sizes between 72 ± 23.8 nm and 90 ± 25.5 nm). For a totally novel approach in EV research, we introduced and

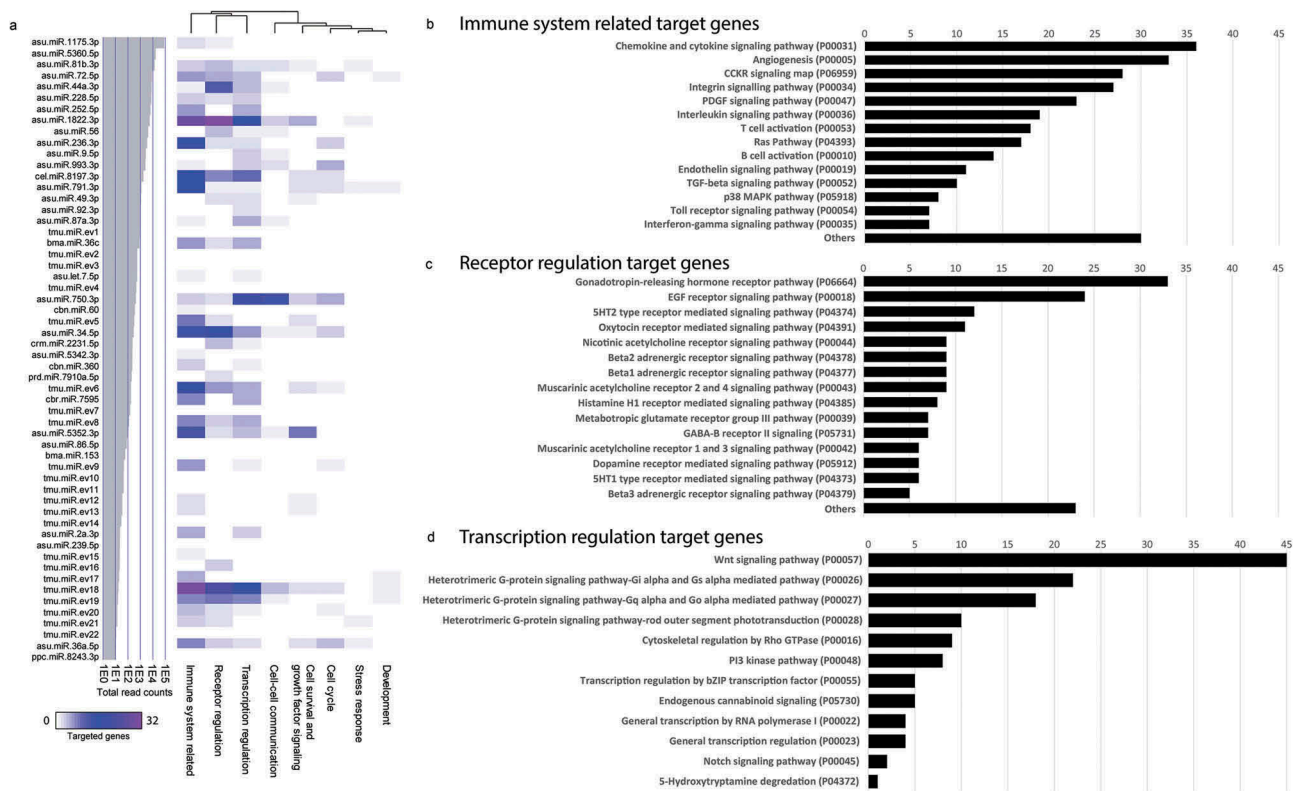


Figure 6. Prediction of *T. muris* extracellular vesicle (EV) miRNA target interactions to murine host genes. Functional map of *T. muris* EV miRNAs and their target murine host genes. (a) Individual targeted host genes are categorized by PantherDB signalling pathway analysis (heat map corresponds to individual targeted genes in the murine host). Bottom axis shows the 56 identified miRNAs in *T. muris* EVs and their abundances (average mean read counts from two biological replicates), termed according to their closest homologues (*de novo* transcripts were designated as tmu.miR.ev#). Total number of targeted genes identified by PantherDB categories classified as (b) “immune system related”, (c) “receptor regulation” and (d) “transcription regulation”.

established a long-term primary *in vitro* culture to generate 3D intestinal organoids, recapitulating the *in vivo* epithelial tissue organization and representing the complete census of progenitors (stem cells) and differentiated cells [22,54]. Although there are colonic cancer cell lines available, such as the intestinal epithelial cell line Caco2, cell lines cannot recapitulate the complex spatial organization of the intestinal epithelium, they have undergone significant molecular changes to become immortal, and they do not represent all intestinal subsets [55]. Hence, we used colonic organoids corresponding to the epithelial barrier, which is the first line of defence against intestinal pathogens. In a first attempt to study whipworm EV interactions with the host intestinal epithelial barrier, we observed vesicle uptake only in a subset of cells. This could not be confirmed by repeating the experiment and analysing the cells by laser scanning confocal imaging and z-stack rendering. At first glance, this suggests that parasite EV uptake – at least under the tested conditions – is a cell-type-unspecific process. Results from several studies show that fluorescently labelled EVs can be taken up by different cell types, whereas other studies indicate that vesicular uptake

is a highly cell-type-specific process [56]. As we do not know which intestinal cells are presented in the screened murine colonic organoids, further studies should include good host cell markers to distinguish the different cells in the heterogeneous organoid system. Furthermore, as the tested conditions could correspond to a high parasite burden present in severe infections, titration of the administered EV dosages and inclusion of different endocytosis-inhibitors could give clues about the specificity and mechanisms of *T. muris* EV–host interactions. In line with the observation of different studies, uptake of EVs was dramatically reduced when incubating at 4°C, suggesting that internalization is not a passive process occurring in metabolically inactive cells and hence relies on some source of energy [57–60]. A disadvantage of the intestinal organoid culture is the lack of any immune cells. Co-culture experiments with intestinal organoids and intraepithelial lymphocytes as described by Nozaki and colleagues [61] could be a powerful tool to study interactions of EVs with immune cells at their primary interface, complemented with host cell proteomics to detect host and parasite proteins, and transcriptomic studies.

The proteomic analysis of the exosome-like EVs showed a total of 381 proteins (364 from *T. muris* and 17 from the host), 130 of which have also been found in the crude ES prep. From the common proteins, only 54 (41.5%) were predicted to have a signal peptide; thus, EVs could be a potential mechanism by which these proteins are secreted by helminths into the extracellular milieu, addressing an issue that has been frequently debated in the literature [8]. It is interesting to note that one tetraspanin (TMUE_s0037005100) was detected in the *T. muris* EVs. Tetraspanins are considered a molecular marker of exosomes, since they are present on the surface membrane of EVs from many different organisms including mammalian cells and bacteria [62]. EVs secreted by or shed from the surface of parasitic trematodes are enriched in tetraspanins [18,21,63], although, in the case of nematodes, they are not abundant on the surface of EVs. For instance, only one member of this family was found in the EVs secreted by the nematode *H. polygyrus* [20]. Since tetraspanins are involved in the formation of the membrane of EVs [62], it is unclear why EVs secreted by nematode parasites are not replete in tetraspanins, as happens in trematodes. In trematodes, exosomes derive from the tegumental syncytium of the worm [64], whereas in nematodes they seem to have an intestinal origin [20]. This different origin could be the reason why tetraspanins are not enriched in nematode EVs. Our dataset presents other proteins usually found in parasitic exosomes, such as 14-3-3, HSP 90 and myoglobin.

Proteins involved in proteolysis were abundantly represented (12.3% of sequences) in the *T. muris* EVs (e.g. trypsin-like, cathepsins and aminopeptidases). *Trichuris* lacks the muscular pharynx that many other nematodes use to ingest their food, a challenging process given the hydrostatic pressure of the pseudocoelom that characterizes the phylum. Instead, it has been suggested that the parasite secretes copious quantities of digestive enzymes for this purpose [8]. We have shown that proteases are heavily represented in the ES products, and proteolysis is also in the top three main GO terms found when we analysed the proteins present in the EVs. Indeed, 37 of the 364 proteins from *T. muris* found in the EVs contain a trypsin or trypsin-like domain. These proteins could be involved in extracellular digestion, and, since feeding is a key process in parasite biology, they might also be potential targets for vaccines and drugs against the parasite. Helminth proteases have also been hypothesized to be involved in immunomodulatory processes, where they degrade important immune cell surface receptors [65] and host intestinal mucins [9,66]. If this is the case, *Trichuris* could be secreting EVs containing peptidases to promote an optimal environment for attaching to the mucosa and feeding purposes.

Proteins containing an SCP/TAPS domain were identified in the EVs secreted by *T. muris*. This family of proteins is abundantly expressed by parasitic nematodes and trematodes. For instance, they represent 35% of the ES products of the hookworm *Ancylostoma caninum* [67] and have been found in free-living and plant nematodes (reviewed by [68]). Their role is still unknown, although they have been suggested to play roles in fundamental biological processes such as larval penetration [69] and modulation of the immune response [70,71], in the transition from the free-living to the parasitic stage [72], and have even been explored as vaccine candidates against hookworm infections [73]. It is interesting to note that EVs from other helminths are enriched for many known vaccine candidate antigens [21]. Since SCP/TAPS proteins are abundant in the EVs secreted by *T. muris*, their potential use as vaccines should be further explored.

We analysed the mRNA and miRNA content of the exosome-like EVs secreted by *T. muris* since it has been well documented that the nucleic acid content of eukaryotic EVs can be delivered between species to other cells and can be functional in the new location [74]. Functional categorization of the 475 mRNAs from *T. muris* EVs revealed a high proportion of protein-binding proteins. Interestingly, mRNAs for common EV proteins were present, including inter alia mRNAs for tetraspanins, HSPs, histones, ubiquitin-related proteins, and signalling- and vesicle trafficking molecules (rab, rho and ras). A significant number of domains found in the proteins predicted from mRNA sequences were involved in reverse transcription and retrotransposon activity, suggesting a strong involvement of these mRNAs in direct interactions with the host target cell genome. This is supported by the hypothesis of shared pathways between EV biogenesis and retrovirus budding, including the molecular composition of the released particles, sites of budding in different cell types and the targeting signals that deliver proteins [75–78].

To gain a more comprehensive picture of the RNA composition of the *T. muris* EVs, we sequenced the miRNAs present in *T. muris* EVs and identified 56 miRNAs, including 22 novel miRNAs without described homology to other nematodes. We also identified miRNAs that shared homology with those from other parasitic nematodes, such as let-7, miR-2, miR-9, miR-34, miR-36 (a and c), miR-44, miR-60, miR-72, miR-81, miR-86, miR-87, miR-92, miR-228, miR-236 and miR-252 [79]. This suggests that secretion of miRNAs by parasitic nematodes is most probably conserved and that EVs could be playing an important role in this secretory pathway. *T. muris* miRNAs that regulate expression of genes involved in specific conditions and cellular pathways were identified. In humans,

more than 60% of all protein-coding genes are thought to be controlled by miRNAs [80]. Our *in silico* prediction analysis of murine host gene interactions of *T. muris* EV miRNAs points towards a strong involvement of parasite miRNAs in regulation/modulation of the host immune system [81]. In this sense, it has been previously demonstrated that small EVs secreted by *H. polygyrus* interact with intestinal epithelial cells of its murine host and suppress type 2 innate immune responses, promoting parasite survival [20]. Similarly, other studies demonstrated the secretion of EVs containing miRNAs by larvae of the porcine whipworm *T. suis*, and although the miRNAs were not sequenced, the authors suggested a possible role in immune evasion [50].

The mechanisms by which parasitic helminths pack their nucleic acid cargo into EVs is still unknown, and, while we hypothesize that an active mechanism might regulate this process, we cannot discard the possibility that mRNAs and miRNAs could be internalized at random. Understanding this mechanism will be of importance in understanding the intimately interactive nature of host–parasite biology. For example, are mRNAs in parasite EVs translated into protein by target host cells, akin to viral hijacking of host cell protein manufacturing machinery? Or, are EV mRNAs unimportant, and is manipulation of host cell gene expression mostly due to miRNAs?

In the present study, we have provided important information regarding the molecules secreted by the murine whipworm *T. muris*. The identification of the secreted proteins and EVs (including their proteomic and RNA content) will prove useful not only for the design of novel approaches aimed at controlling whipworm infections, but also to understand the way the parasite promotes an optimal environment for its survival.

Disclosure statement

No potential conflict of interest was reported by the authors.

Funding

This work was supported by a programme grant from the National Health and Medical Research Council (NHMRC) [programme grant number 1037304] and a Principal Research fellowship from NHMRC to AL. RME was supported by an Early Postdoc.Mobility fellowship (P2ZHP3_161693) from the Swiss National Science Foundation. MHT was supported by an Endeavour Research Fellowship. The funders had no role in the study design, data collection and analysis, decision to publish or preparation of the manuscript. The authors declare no competing financial interests. Schweizerischer Nationalfonds zur

Förderung der Wissenschaftlichen Forschung [P2ZHP3_161693].

ORCID

Ramon M. Eichenberger  <http://orcid.org/0000-0002-9337-9616>

Md Hasanuzzaman Talukder  <http://orcid.org/0000-0001-9538-2520>

Matthew A. Field  <http://orcid.org/0000-0003-0788-6513>

Phurpa Wangchuk  <http://orcid.org/0000-0002-4381-7382>

Alex Loukas  <http://orcid.org/0000-0002-0896-8441>

Javier Sotillo  <http://orcid.org/0000-0002-1443-7233>

References

- [1] Bethony J, Brooker S, Albonico M, et al. Soil-transmitted helminth infections: ascariasis, trichuriasis, and hookworm. *Lancet*. 2006 May 06;367(9521):1521–1532. PubMed PMID: 16679166.
- [2] Pullan RL, Smith JL, Jasrasaria R, et al. Global numbers of infection and disease burden of soil transmitted helminth infections in 2010. *Parasit Vectors*. 2014 Jan 21;7:37. PubMed PMID: 24447578; PubMed Central PMCID: PMC3905661.
- [3] Klementowicz JE, Travis MA, Grecis RK. *Trichuris muris*: a model of gastrointestinal parasite infection. *Semin Immunopathol*. 2012 Nov;34(6):815–828. PubMed PMID: 23053395; PubMed Central PMCID: PMC3496546.
- [4] Cliffe LJ, Grecis RK. The *Trichuris muris* system: a paradigm of resistance and susceptibility to intestinal nematode infection. *Adv Parasitol*. 2004;57:255–307. PubMed PMID: 15504540.
- [5] Bancroft AJ, Hayes KS, Grecis RK. Life on the edge: the balance between macrofauna, microflora and host immunity. *Trends Parasitol*. 2012 Mar;28(3):93–98. PubMed PMID: 22257556.
- [6] Hurst RJ, Else KJ. *Trichuris muris* research revisited: a journey through time. *Parasitology*. 2013 Sep;140(11):1325–1339. PubMed PMID: 23965819; PubMed Central PMCID: PMC3761323.
- [7] Grecis RK, Bancroft AJ. Interleukin-13: a key mediator in resistance to gastrointestinal-dwelling nematode parasites. *Clin Rev Allergy Immunol*. 2004 Feb;26(1):51–60. PubMed PMID: 14755075.
- [8] Foth BJ, Tsai IJ, Reid AJ, et al. Whipworm genome and dual-species transcriptome analyses provide molecular insights into an intimate host-parasite interaction. *Nat Genet*. 2014 Jul;46(7):693–700. PubMed PMID: 24929830; PubMed Central PMCID: PMC35012510.
- [9] Hasnain SZ, McGuckin MA, Grecis RK, et al. Serine protease(s) secreted by the nematode *Trichuris muris* degrade the mucus barrier. *PLoS Negl Trop Dis*. 2012;6(10):e1856. PubMed PMID: 23071854; PubMed Central PMCID: PMC3469553.
- [10] Laan LC, Williams AR, Stavenhagen K, et al. The whipworm (*Trichuris suis*) secretes prostaglandin E2 to suppress proinflammatory properties in human dendritic cells. *Faseb J*. 2016 Nov 02 PubMed PMID: 27806992.

- [11] Ditgen D, Anandarajah EM, Hansmann J, et al. Multifunctional thioredoxin-like protein from the gastrointestinal parasitic nematodes *strongyloides ratti* and *trichuris suis* affects mucosal homeostasis. *J Parasitol Res.* 2016;2016:1–17. PubMed PMID: 27872753.
- [12] Santos LN, Gallo MB, Silva ES, et al. A proteomic approach to identify proteins from *Trichuris trichiura* extract with immunomodulatory effects. *Parasite Immunol.* 2013 May-Jun;35(5–6):188–193. PubMed PMID: 23398517.
- [13] Drake LJ, Barker GC, Korchev Y, et al. Molecular and functional characterization of a recombinant protein of *Trichuris trichiura*. *Proc Biol Sci.* 1998 Aug 22;265(1405):1559–1565. PubMed PMID: 9744108; PubMed Central PMCID: PMCPMC1689327.
- [14] Drake L, Korchev Y, Bashford L, et al. The major secreted product of the whipworm, *Trichuris*, is a pore-forming protein. *Proc Biol Sci.* 1994 Sep 22;257(1350):255–261. PubMed PMID: 7991635.
- [15] Marcilla A, Trellis M, Cortes A, et al. Extracellular vesicles from parasitic helminths contain specific excretory/secretory proteins and are internalized in intestinal host cells. *PLoS One.* 2012;7(9):e45974. PubMed PMID: 23029346; PubMed Central PMCID: PMCPMC3454434.
- [16] Marcilla A, Martin-Jaular L, Trellis M, et al. Extracellular vesicles in parasitic diseases. *J Extracell Vesicles.* 2014;3:25040. PubMed PMID: 25536932; PubMed Central PMCID: PMCPMC4275648.
- [17] Coakley G, Maizels RM, Buck AH. Exosomes and other extracellular vesicles: the new communicators in parasite infections. *Trends Parasitol.* 2015 Oct;31(10):477–489. PubMed PMID: 26433251; PubMed Central PMCID: PMCPMC4685040.
- [18] Chaiyadet S, Sotillo J, Smout M, et al. Carcinogenic liver fluke secretes extracellular vesicles that promote cholangiocytes to adopt a tumorigenic phenotype. *J Infect Dis.* 2015 Nov 15;212(10):1636–1645. PubMed PMID: 25985904; PubMed Central PMCID: PMCPMC4621255.
- [19] Wang L, Li Z, Shen J, et al. Exosome-like vesicles derived by *Schistosoma japonicum* adult worms mediates M1 type immune-activity of macrophage. *Parasitol Res.* 2015 May;114(5):1865–1873. PubMed PMID: 25855345.
- [20] Buck AH, Coakley G, Simbari F, et al. Exosomes secreted by nematode parasites transfer small RNAs to mammalian cells and modulate innate immunity. *Nat Commun.* 2014 Nov 25;5:5488. PubMed PMID: 25421927; PubMed Central PMCID: PMCPMC4263141.
- [21] Sotillo J, Pearson M, Potriquet J, et al. Extracellular vesicles secreted by *Schistosoma mansoni* contain protein vaccine candidates. *Int J Parasitol.* 2016 Jan;46(1):1–5. PubMed PMID: 26460238.
- [22] Sato T, Stange DE, Ferrante M, et al. Long-term expansion of epithelial organoids from human colon, adenoma, adenocarcinoma, and Barrett's epithelium. *Gastroenterology.* 2011 Nov;141(5):1762–1772. PubMed PMID: 21889923.
- [23] Sage D, Donati L, Soulez F, et al. DeconvolutionLab2: an open-source software for deconvolution microscopy. *Methods.* 2017 Feb 15;115:28–41. PubMed PMID: 28057586.
- [24] Sotillo J, Sanchez-Flores A, Cantacessi C, et al. Secreted proteomes of different developmental stages of the gastrointestinal nematode *Nippostrongylus brasiliensis*. *Mol Cell Proteomics.* 2014 Oct;13(10):2736–2751. PubMed PMID: 24994561; PubMed Central PMCID: PMCPMC4188999.
- [25] Vaudel M, Barsnes H, Berven FS, et al. SearchGUI: an open-source graphical user interface for simultaneous OMSSA and X!Tandem searches. *Proteomics.* 2011 Mar;11(5):996–999. PubMed PMID: 21337703.
- [26] Vaudel M, Burkhart JM, Zahedi RP, et al. PeptideShaker enables reanalysis of MS-derived proteomics data sets. *Nat Biotechnol.* 2015 Jan;33(1):22–24. PubMed PMID: 25574629.
- [27] Gotz S, Garcia-Gomez JM, Terol J, et al. High-throughput functional annotation and data mining with the Blast2GO suite. *Nucleic Acids Res.* 2008 Jun;36(10):3420–3435. PubMed PMID: 18445632; PubMed Central PMCID: PMCPMC2425479.
- [28] Finn RD, Clements J, Arndt W, et al. HMMER web server: 2015 update. *Nucleic Acids Res.* 2015 Jul 01;43(W1):W30–38. PubMed PMID: 25943547; PubMed Central PMCID: PMCPMC4489315.
- [29] Marchler-Bauer A, Lu S, Anderson JB, et al. CDD: a conserved domain database for the functional annotation of proteins. *Nucleic Acids Res.* 2011 Jan;39:D225–229. PubMed PMID: 21109532; PubMed Central PMCID: PMCPMC3013737.
- [30] Petersen TN, Brunak S, Von Heijne G, et al. SignalP 4.0: discriminating signal peptides from transmembrane regions. *Nat Methods.* 2011 Sep 29;8(10):785–786. PubMed PMID: 21959131.
- [31] Howe KL, Bolt BJ, Cain S, et al. WormBase 2016: expanding to enable helminth genomic research. *Nucleic Acids Res.* 2016 Jan 04;44(D1):D774–780. PubMed PMID: 26578572; PubMed Central PMCID: PMCPMC4702863.
- [32] Dobin A, Davis CA, Schlesinger F, et al. STAR: ultrafast universal RNA-seq aligner. *Bioinformatics.* 2013 Jan 01;29(1):15–21. PubMed PMID: 23104886; PubMed Central PMCID: PMCPMC3530905.
- [33] Schmiieder R, Lim YW, Edwards R. Identification and removal of ribosomal RNA sequences from metatranscriptomes. *Bioinformatics.* 2012 Feb 01;28(3):433–435. PubMed PMID: 22155869; PubMed Central PMCID: PMCPMC3268242.
- [34] Altschul SF, Madden TL, Schaffer AA, et al. Gapped BLAST and PSI-BLAST: a new generation of protein database search programs. *Nucleic Acids Res.* 1997 Sep 01;25(17):3389–3402. PubMed PMID: 9254694; PubMed Central PMCID: PMCPMC146917.
- [35] Friedlander MR, Mackowiak SD, Li N, et al. miRDeep2 accurately identifies known and hundreds of novel microRNA genes in seven animal clades. *Nucleic Acids Res.* 2012 Jan;40(1):37–52. PubMed PMID: 21911355; PubMed Central PMCID: PMCPMC3245920.
- [36] Kozomara A, Griffiths-Jones S. miRBase: annotating high confidence microRNAs using deep sequencing data. *Nucleic Acids Res.* 2014 Jan;42(Database issue):D68–73. PubMed PMID: 24275495; PubMed Central PMCID: PMCPMC3965103.

- [37] Enright AJ, John B, Gaul U, et al. MicroRNA targets in *Drosophila*. *Genome Biol.* 2003;5(1):R1. PubMed PMID: 14709173; PubMed Central PMCID: PMCPMC395733.
- [38] Yates A, Akanni W, Amode MR, et al. Ensembl 2016. *Nucleic Acids Res.* 2016 Jan 04;44(D1):D710–716. PubMed PMID: 26687719; PubMed Central PMCID: PMCPMC4702834.
- [39] Mi H, Huang X, Muruganujan A, et al. PANTHER version 11: expanded annotation data from Gene Ontology and Reactome pathways, and data analysis tool enhancements. *Nucleic Acids Res.* 2016 Nov 29 PubMed PMID: 27899595.
- [40] Fabregat A, Sidiropoulos K, Garapati P, et al. The reactome pathway knowledgebase. *Nucleic Acids Res.* 2016 Jan 04;44(D1):D481–487. PubMed PMID: 26656494; PubMed Central PMCID: PMCPMC4702931.
- [41] Webber J, Clayton A. How pure are your vesicles? *J Extracell Vesicles.* 2013;2:19861. PubMed PMID: 24009896; PubMed Central PMCID: PMCPMC3760653.
- [42] WHO. Preventive chemotherapy in human helminthiasis: coordinated use of anthelmintic drugs in control interventions: a manual for health professionals and programme managers. 2006. Available from: http://whqlibdoc.who.int/publications/2006/9241547103_eng.pdf.
- [43] Stephenson LS, Holland CV, Cooper ES. The public health significance of *Trichuris trichiura*. *Parasitology.* 2000;121 Suppl:S73–95. PubMed PMID: 11386693.
- [44] WHO. Deworming for health and development. Report of the third global meeting of the partners for parasite control. Geneva: World Health Organization; 2005.
- [45] Anonymous. Schistosomiasis and soil-transmitted helminth infections (World Health Assembly Resolution WHA54.19). 2001. Available from: http://apps.who.int/gb/archive/pdf_files/WHA54/ea54r19.pdf.
- [46] Williams SE, Brown TI, Roghanian A, et al. SLPI and elafin: one glove, many fingers. *Clin Sci (Lond).* 2006 Jan;110(1):21–35. PubMed PMID: 16336202.
- [47] Scott A, Weldon S, Taggart CC. SLPI and elafin: multifunctional antiproteases of the WFDC family. *Biochem Soc Trans.* 2011 Oct;39(5):1437–1440. PubMed PMID: 21936829.
- [48] Wilkinson TS, Roghanian A, Simpson AJ, et al. WAP domain proteins as modulators of mucosal immunity. *Biochem Soc Trans.* 2011 Oct;39(5):1409–1415. PubMed PMID: 21936824.
- [49] Cantacessi C, Campbell BE, Visser A, et al. A portrait of the “SCP/TAPS” proteins of eukaryotes—developing a framework for fundamental research and biotechnological outcomes. *Biotechnol Adv.* 2009 Jul-Aug;27(4):376–388. PubMed PMID: 19239923.
- [50] Hansen EP, Kringel H, Williams AR, et al. Secretion of RNA-containing extracellular vesicles by the porcine whipworm, *Trichuris suis*. *J Parasitol.* 2015 Jun;101(3):336–340. PubMed PMID: 25723295.
- [51] Liegeois S, Benedetto A, Garnier JM, et al. The V0-ATPase mediates apical secretion of exosomes containing Hedgehog-related proteins in *Caenorhabditis elegans*. *J Cell Biol.* 2006 Jun 19;173(6):949–961. PubMed PMID: 16785323; PubMed Central PMCID: PMCPMC2063919.
- [52] Tritten L, Clarke D, Timmins S, et al. *Dirofilaria immitis* exhibits sex- and stage-specific differences in excretory/secretory miRNA and protein profiles. *Vet Parasitol.* 2016 Dec 15;232:1–7. PubMed PMID: 27890076.
- [53] Zamanian M, Fraser LM, Agbedanu PN, et al. Release of small RNA-containing exosome-like vesicles from the human filarial parasite *Brugia malayi*. *PLoS Negl Trop Dis.* 2015;9(9):e0004069. PubMed PMID: 26401956; PubMed Central PMCID: PMCPMC4581865.
- [54] Sato T, Clevers H. Growing self-organizing mini-guts from a single intestinal stem cell: mechanism and applications. *Science.* 2013 Jun 7;340(6137):1190–1194. PubMed PMID: 23744940.
- [55] Frising UC, Stange J, Veldhoen M, editors. Intestinal organoids - a powerful model to study interactions of the epithelial barrier with its environment. Proceedings of the British conference of undergraduate research; 2014; University of Nottingham, UK.
- [56] Mulcahy LA, Pink RC, Carter DR. Routes and mechanisms of extracellular vesicle uptake. *J Extracell Vesicles.* 2014;3. PubMed PMID: 25143819; PubMed Central PMCID: PMCPMC4122821.
- [57] Escreve C, Keller S, Altevogt P, et al. Interaction and uptake of exosomes by ovarian cancer cells. *BMC Cancer.* 2011 Mar 27;11:108. PubMed PMID: 21439085; PubMed Central PMCID: PMCPMC3072949.
- [58] Zech D, Rana S, Buchler MW, et al. Tumor-exosomes and leukocyte activation: an ambivalent crosstalk. *Cell Commun Signal.* 2012 Nov 28;10(1):37. PubMed PMID: 23190502; PubMed Central PMCID: PMCPMC3519567.
- [59] Tian T, Zhu YL, Hu FH, et al. Dynamics of exosome internalization and trafficking. *J Cell Physiol.* 2013 Jul;228(7):1487–1495. PubMed PMID: 23254476.
- [60] Christianson HC, Svensson KJ, Van Kuppevelt TH, et al. Cancer cell exosomes depend on cell-surface heparan sulfate proteoglycans for their internalization and functional activity. *Proc Natl Acad Sci U S A.* 2013 Oct 22;110(43):17380–17385. PubMed PMID: 24101524; PubMed Central PMCID: PMCPMC3808637.
- [61] Nozaki K, Mochizuki W, Matsumoto Y, et al. Co-culture with intestinal epithelial organoids allows efficient expansion and motility analysis of intraepithelial lymphocytes. *J Gastroenterol.* 2016 Mar;51(3):206–213. 10.1007/s00535-016-1170-8. PubMed PMID: 26800996; PubMed Central PMCID: PMCPMC4771822.
- [62] Andreu Z, Yanez-Mo M. Tetraspanins in extracellular vesicle formation and function. *Front Immunol.* 2014;5:442. PubMed PMID: 25278937; PubMed Central PMCID: PMCPMC4165315.
- [63] Cwiklinski K, de la Torre-Escudero E, Trelis M, et al. The extracellular vesicles of the helminth pathogen, *Fasciola hepatica*: biogenesis pathways and cargo molecules involved in parasite pathogenesis. *Mol Cell Proteomics.* 2015 Dec;14(12):3258–3273. PubMed PMID: 26486420; PubMed Central PMCID: PMCPMC4762619.
- [64] de la Torre-Escudero E, Bennett AP, Clarke A, et al. Extracellular vesicle biogenesis in helminths: more than one route to the surface? *Trends Parasitol.* 2016 Dec;32(12):921–929. PubMed PMID: 27720334.

- [65] Nishikado H, Fujimura T, Taka H, et al. Cysteine protease antigens cleave CD123, the alpha subunit of murine IL-3 receptor, on basophils and suppress IL-3-mediated basophil expansion. *Biochem Biophys Res Commun.* 2015 May 01;460(2):261–266. PubMed PMID: 25778870.
- [66] Drake LJ, Bianco AE, Bundy DA, et al. Characterization of peptidases of adult *Trichuris muris*. *Parasitology.* 1994 Dec;109(Pt 5):623–630. PubMed PMID: 7831097.
- [67] Morante T, Shepherd C, Constantinoiu C, et al. Revisiting the *Ancylostoma Caninum* secretome provides new information on hookworm-host interactions. *Proteomics.* 2017 Oct 20;17:1700186. PubMed PMID: 29052354.
- [68] Cantacessi C, Gasser RB. SCP/TAPS proteins in helminths-where to from now? *Mol Cell Probes.* 2012 Feb;26(1):54–59. PubMed PMID: 22005034.
- [69] Wu X-J, Sabat G, Brown JF, et al. Proteomic analysis of *Schistosoma mansoni* proteins released during in vitro miracidium-to-sporocyst transformation. *Mol Biochem Parasitol.* 2009 Mar;164(1):32–44. PubMed PMID: 19095013; PubMed Central PMCID: PMCPCMC2665799.
- [70] Chen J, Hu X, He S, et al. Expression and immune response analysis of *Schistosoma japonicum* VAL-1, a homologue of vespid venom allergens. *Parasitol Res.* 2010 May;106(6):1413–1418. PubMed PMID: 20306204.
- [71] Tribolet L, Cantacessi C, Pickering DA, et al. Probing of a human proteome microarray with a recombinant pathogen protein reveals a novel mechanism by which hookworms suppress B-cell receptor signaling. *J Infect Dis.* 2015 Feb 01;211(3):416–425. PubMed PMID: 25139017.
- [72] Moser JM, Freitas T, Arasu P, et al. Gene expression profiles associated with the transition to parasitism in *Ancylostoma caninum* larvae. *Mol Biochem Parasitol.* 2005 Sep;143(1):39–48. PubMed PMID: 15979737.
- [73] Loukas A, Bethony J, Brooker S, et al. Hookworm vaccines: past, present, and future. *Lancet Infect Dis.* 2006 Nov;6(11):733–741. PubMed PMID: 17067922.
- [74] Valadi H, Ekstrom K, Bossios A, et al. Exosome-mediated transfer of mRNAs and microRNAs is a novel mechanism of genetic exchange between cells. *Nat Cell Biol.* 2007 Jun;9(6):654–659. PubMed PMID: 17486113.
- [75] Nguyen DG, Booth A, Gould SJ, et al. Evidence that HIV budding in primary macrophages occurs through the exosome release pathway. *J Biol Chem.* 2003 Dec 26;278(52):52347–52354. PubMed PMID: 14561735; eng.
- [76] Fang Y, Wu N, Gan X, et al. Higher-order oligomerization targets plasma membrane proteins and HIV gag to exosomes. *PLoS Biol.* 2007 Jun;5(6):e158. PubMed PMID: 17550307; PubMed Central PMCID: PMCPCMC1885833.
- [77] Krishnamoorthy L, Bess JW Jr., Preston AB, et al. HIV-1 and microvesicles from T cells share a common glycome, arguing for a common origin. *Nat Chem Biol.* 2009 Apr;5(4):244–250. PubMed PMID: 19234452; PubMed Central PMCID: PMCPCMC2713040.
- [78] Shen B, Wu N, Yang JM, et al. Protein targeting to exosomes/microvesicles by plasma membrane anchors. *J Biol Chem.* 2011 Apr 22;286(16):14383–14395. PubMed PMID: 21300796; PubMed Central PMCID: PMCPCMC3077638.
- [79] Cai J, Han Y, Ren H, et al. Extracellular vesicle-mediated transfer of donor genomic DNA to recipient cells is a novel mechanism for genetic influence between cells. *J Mol Cell Biol.* 2013 Aug;5(4):227–238. PubMed PMID: 23580760; PubMed Central PMCID: PMCPCMC3733418.
- [80] Daugaard I, Hansen TB. Biogenesis and function of ago-associated RNAs. *Trends Genet.* 2017 Feb 04;33:208–219.
- [81] McSorley HJ, Loukas A. The immunology of human hookworm infections. *Parasite Immunol.* 2010 Aug;32(8):549–559. PubMed PMID: 20626810.